Coordination Chemistry of Trivalent Lanthanide and Actinide Ions in Dilute and Concentrated Chloride Solutions

P. G. Allen,*,†,‡ J. J. Bucher,† D. K. Shuh,† N. M. Edelstein,† and I. Craig†

Actinide Chemistry Group, Chemical Sciences Division, Lawrence Berkeley National Laboratory, Berkeley, California 94720, and Seaborg Institute for Transactinium Science, Lawrence Livermore National Laboratory, Livermore, California 94551

Received May 24, 1999

We have used EXAFS spectroscopy to investigate the inner sphere coordination of trivalent lanthanide (Ln) and actinide (An) ions in aqueous solutions as a function of increasing chloride concentration. At low chloride concentration, the hydration numbers and corresponding Ln,An−O bond lengths are as follows: La^{3+}, $N = 9.2$, $R = 2.54$ Å; Ce^{3+}, $N = 9.3$, $R = 2.52$ Å; Nd^{3+}, $N = 9.5$, $R = 2.49$ Å; Eu^{3+}, $N = 9.3$, $R = 2.43$ Å; Yb^{3+}, $N = 8.7$, $R = 2.32$ Å; Y^{3+}, $N = 9.7$, $R = 2.36$ Å; Am^{3+}, $N = 10.3$, $R = 2.48$ Å; Cm^{3+}, $N = 10.2$, $R = 2.45$ Å. In ca. 14 M LiCl, the early Ln^{3+} ions (La, Ce, Nd, and Eu) show inner sphere Cl^- complexation along with a loss of H_2O. The average chloride coordination numbers and Ln−Cl bond lengths are as follows: La^{3+}, $N = 2.1$, $R = 2.92$ Å; Ce^{3+}, $N = 1.8$, $R = 2.89$ Å; Nd^{3+}, $N = 1.9$, $R = 2.85$ Å; Eu^{3+}, $N = 1.1$, $R = 2.81$ Å. The extent of Cl^- ion complexation decreases going across the Ln^{3+} series to the point where Yb^{3+} shows no Cl^- complexation and no loss of coordinated water molecules. The actinide ions, Am^{3+} and Cm^{3+}, show the same structural effects as the early Ln^{3+} ions, i.e., Cl^- ion replacement of the H_2O at high chloride thermodynamic activities. The Cl^- ion coordination numbers and An−Cl bond lengths are: Am^{3+}, $N = 1.8$, $R = 2.81$ Å; Cm^{3+}, $N = 2.4$, $R = 2.76$ Å. When combined with results reported previously for Pu^{3+} which showed no significant chloride complexation in 12 M LiCl, these results suggest that the extent of chloride complexation is increasing across the An^{3+} series. The origin of the differences in chloride complex formation between the Ln^{3+} and An^{3+} ions and the relevance to earlier work is discussed.

Introduction

The identification of Cl^- complexes of the trivalent actinides (An^{3+}) and lanthanides (Ln^{3+}) has been the subject of numerous investigations because of their importance in actinide separations and in processing chemistry. Actinide chloride complexes also may be formed in nuclear waste repositories located in bedded salt formations where information on the possible species present is needed for modeling of actinide transport. Many techniques have been utilized to determine stability constants (quotients) with tracer and macro quantities of lanthanide and actinide materials and with various concentrations of electrolytes. The stability constants for the chloro complexes Ln^{3+} and An^{3+} have been collected in a number of reviews.[1−5] Tabulated values for the stability constants show considerable variation due in large part to differences in experimental conditions and problems from the interpretation and comparison of data obtained by different techniques.[6] For example, solvent extraction and ion exchange methods frequently cannot distinguish between the formation of inner sphere or outer sphere complexes. On the other hand, spectroscopic methods are known to be sensitive primarily to inner sphere or local field effects.[7−11]

In a series of papers Shiloh and Marcus reported spectrophotometric studies of U^{3+}, Np^{3+}, Pu^{3+}, and Am^{3+} ions in concentrated aqueous LiCl solutions.[12−14] From these data they derived chloride stability constants which they attributed to inner sphere chloro complexes for these trivalent actinide ions. However, Fuger et al. in their review of aqueous inorganic complexes of the actinides commented that stability constants obtained at high LiCl concentrations should not be directly compared with other data since the water activity in these solutions is drastically lowered with the consequent altering of the hydration sphere about the metal ion.[15]

† Lawrence Berkeley National Laboratory.
‡ Lawrence Livermore National Laboratory.

(1) (a) Sillén, L. G.; Martell, A. E. *Stability Constants of Metal-Ion Complexes*; Spec. Publ. No. 17; The Chemical Society: London, 1964; (b) Spec. Publ. No. 25; The Chemical Society: London, 1971. (c) Smith, R. M.; Martell, A. E. *Critical Stability Constants, Volume 4: Inorganic Complexes*; Plenum Press: New York, 1976.
(2) Ahrland, S. In *The Chemistry of the Actinide Elements*; Katz, J. J., Seaborg, G. T., Morss, L. R., Eds.; Chapman and Hall: New York, 1986; Vol. 2, p 1498.
(3) Degischer, G.; Choppin, G. R. In *Gmelin Handbuch der Anorganische Chemie, Transuranium*, Part D1: Chemie in Lösung, (Suppl. Vol. 20); Springer-Verlag: Berlin, 1975; p 129.
(4) Fuger, J.; Khodakovsky, I. L.; Sergeyeva, E. I.; Medvedev, V. A.; Navratil, J. D. *The Chemical Thermodynamics of Actinide Elements and Compounds Part 12: The Actinide Aqueous Inorganic Complexes*; IAEA: Vienna, 1992.
(5) Fanghänel, T.; Kim, J. I.; Klenze, R.; Kato, Y. *J. Alloys Compd* **1995**, *225*, 308−311.
(6) Choppin, G. R. *J. Alloys Compd* **1997**, *249*, 9−13.
(7) Choppin, G. R.; Henrie, D. E.; Buijs, K. *Inorg. Chem.* **1966**, *5*, 1747.
(8) Rinaldi, P. L.; Khan, S. A.; Choppin, G. R.; Levy, G. C. *J. Am. Chem. Soc.* **1979**, *101*, 1350.
(9) Breen, P. J.; Horrocks, W. D., Jr. *Inorg. Chem.* **1983**, *22*, 536.
(10) Lockhead, M. J.; Wamsley, P. R.; Bray, K. L. *Inorg. Chem.* **1994**, *33*, 2000.
(11) Choppin, G. R.; Wang, Z. M. *Inorg. Chem.* **1997**, *36*, 249.
(12) Shiloh, M.; Marcus, Y. *Isr. J. Chem.* **1965**, *3*, 123.
(13) Shiloh, M.; Marcus, Y. *J. Inorg. Nucl. Chem.* **1966**, *28*, 2725.
(14) Marcus, Y.; Shiloh, M. *Isr. J. Chem.* **1969**, *7*, 31.
(15) Reference 4, page 66.

10.1021/ic9905953 CCC: $19.00
Published on Web 01/20/2000

A substantial amount of information has been obtained from neutron,[16−18] X-ray,[19−21] and UV−visible absorption[22,23] studies. These studies indicate that, in acidic aqueous solution, the number of coordinated water molecules (hydration number, N_O) decreases from 9 for the early Ln^{3+} ions (La−Nd) to 8 for the heavier Ln^{3+} ions (Tb−Lu). Results from luminescence lifetimes[8,9,24,25] and Raman spectroscopy[26,27] in perchlorate solutions have been interpreted as an anomalous increase in average hydration number with increasing perchlorate concentrations for Eu^{3+} and Gd^{3+} ions. However, the same luminescence and Raman studies give opposite trends for the hydration behavior of Eu^{3+} in the presence of Cl^-. Other studies have used UV−visible absorption[28] for Am^{3+} and luminescence spectroscopy[29,30] for Cm^{3+} and indicate a hydration number of ∼9 for the first coordination sphere. In the absence of detailed structural data, it has been inferred from mobility and conductivity measurements that the changes in the hydration number across the An^{3+} series should be analogous to those observed for the Ln^{3+} series.[31]

Synchrotron-based extended X-ray absorption fine-structure (EXAFS) spectroscopy is a relatively new technique being applied to characterize the structure of actinide complexes in solution. It offers an advantage to other approaches in that it is directly sensitive to inner sphere structure (coordination number and bond length) and measures structure summed over all possible species for a given element (i.e., species are not spectroscopically silent). Disadvantages are that the evaluation of coordination numbers is highly model dependent, such that the precision in an EXAFS measurement of N_O may be within a few percent yet the absolute accuracy may depend more on the modeling technique or assumptions employed. For example, one recent study on the hydration number of Ln^{3+} ions[32] found a change from 9 to 8 across the series consistent with earlier X-ray and neutron measurements. Yet in another carefully detailed EXAFS study, it was concluded that N_O remains constant at a value of 12 over the entire Ln^{3+} series.[33]

In earlier work we determined the Cl^- complexation of representative actinide ions in various oxidation states (UO_2^{2+}, NpO_2^+, Np^{4+}, and Pu^{3+}) as a function of the concentration of Cl^- ion in aqueous solution.[34] One of the most striking results was the lack of inner sphere Cl^- complexation for Pu^{3+} even at very high LiCl concentrations. For this ion in 0.01 M LiCl we find (using $S_0^2 = 1$, see below) 9.2 ± 1.1 water molecules at 2.51 Å. This compares well with the result of 8−9 water molecules at 2.49 Å found by Conradson et al.[35] In 12.3 M LiCl, the oxygen coordination number decreases to 5.2 ± 1.1; however, no inner sphere chloride ion complexation is observed.[34] This result is in contrast with the recently reported formation of inner shell chloride complexes of Cm^{3+} in aqueous $CaCl_2$ solutions which have been characterized by optical spectroscopic techniques.[5] We have complemented our earlier study on Pu^{3+} by including chloride complexation studies with the higher atomic number cations Am^{3+} and Cm^{3+}. For comparison purposes we have also measured some representative lanthanide ions which encompass the entire 4f series and which allow us to compare ions of the two f-element series with comparable ionic radii. Aqueous solutions of Am^{3+} and Cm^{3+} and representative lanthanide ions have been measured using EXAFS spectroscopy as a function of Cl^- ion concentration. The number of H_2O molecules and Cl^- ions for each of the measured metal ion solutions are given, and the results are discussed and compared with previous studies.

Experimental Section

Solution and Sample Preparation. All sample preparations were done using the Actinide Chemistry Group facilities at the Lawrence Berkeley National Laboratory (LBNL). ACS reagent grade anhydrous lithium chloride (Aldrich) and ACS reagent grade concentrated hydrochloric acid (J. T. Baker) were used as received. Deionized water was used for all solution preparations. Lithium chloride solutions were prepared from either a 0.01 or 0.001 M HCl stock solution. Oxides of the Ln^{3+} ions (Ln = La, Ce, Nd, Eu, Yb) and Y^{3+} were obtained from Alfa-Aesar, Inc. ^{243}Am and ^{248}Cm oxides were obtained from Oak Ridge National Laboratory under the auspices of the transplutonium research program of the Department of Energy, Division of Basic Energy Sciences.

Stock solutions of the trivalent lanthanides were made by dissolving a weighed amount of oxide in aqueous HCl, and varied from 2 to 3 M in Ln^{3+} concentration. The lanthanide solutions were placed in thin (2 mil thick) polyethylene bags fabricated for X-ray measurements. For the Am^{3+} and Cm^{3+} solutions, the materials were also dissolved in HCl. Aliquots of these solutions were used to determine the concentration of the stock solutions by α counting, using a NIST traceable reference. The EXAFS samples were prepared by adding the metal ion stock solutions with desired LiCl solutions into 0.4 mL plastic centrifuge tubes (∼5 mm diameter). The final Ln^{3+} and An^{3+} ion concentrations were 0.1 and 0.01 M, respectively. The Ln^{3+} ions were measured in ∼0.2 M HCl and 14 M LiCl solutions. The An^{3+} ions were measured in 0.2 M HCl, and as a function of increasing LiCl concentration ranging from approximately 8 to 12 M. All operations with the transuranium elements were performed in radioactive containment gloveboxes. For safety purposes, the Am^{3+} and Cm^{3+} solutions were sealed in the centrifuge tubes by melting the caps directly onto the plastic body with a soldering iron. Other details regarding the safe handling of radioactive samples as well as the radiological monitoring and controls at SSRL have been described previously.[34]

XAFS Data Acquisition and Analysis. La^{3+}, Ce^{3+}, Nd^{3+}, Eu^{3+}, Yb^{3+}, Am^{3+}, Cm^{3+} $L_{II,III}$-edge and Y^{3+} K-edge X-ray absorption spectra were collected at SSRL on wiggler beamline 4-1 under normal ring operating conditions (3.0 GeV, 50−100 mA). A Si (220) double-crystal monochromator was employed to perform energy scans of the synchrotron X-ray beam. The vertical slit width inside the X-ray hutch was 0.5 mm, which reduces the effects of beam instabilities and monochromator glitches while providing ample photon flux. The higher order harmonic content of the beam was rejected by detuning the crystals in the monochromator so that the incident flux was reduced to 50% of its maximum at the scan ending energy.

All of the Ln^{3+}, An^{3+}, and Y^{3+} solutions were measured in fluorescence mode using a Ge solid state detector developed at Lawrence Berkeley National Laboratory.[36] The detector was operated

(16) Cossy, C.; Barnes, A. C.; Enderby, J. E.; Merbach, A. E. *J. Chem. Phys.* **1989**, *90*, 3254.
(17) Narten, A. H.; Hahn, R. L. *J. Phys. Chem.* **1983**, *87*, 3191.
(18) Annis, B. K.; Hahn, R. L.; Narten, A. H. *J. Chem. Phys.* **1985**, *82*, 2086.
(19) Habenschuss, A.; Spedding, F. H. *J. Chem. Phys.* **1979**, *70*, 2797.
(20) Habenschuss, A.; Spedding, F. H. *J. Chem. Phys.* **1979**, *70*, 3759.
(21) Johansson, G.; Yokoyama, H. *Inorg. Chem.* **1990**, *29*, 2460.
(22) Rajnak, K.; Couture, L. *Chem. Phys.* **1981**, *55*, 331.
(23) Rajnak, K.; Couture, L. *Chem. Phys.* **1984**, *85*, 315.
(24) Lis, S.; Choppin, G. R. *Mater. Chem. Phys.* **1992**, *31*, 159.
(25) Tanaka, F.; Yamashita, S. *Inorg. Chem.* **1984**, *23*, 2044.
(26) Kanno, H.; Hiraishi, J. *J. Phys. Chem.* **1982**, *86*, 1488.
(27) Kanno, H.; Yokoyama, H. *Polyhedron* **1996**, *15*, 1437.
(28) Carnall, W. T. *J. Less-Common Met.* **1989**, *156*, 221.
(29) Beitz, J. V. *Rad. Chim. Acta* **1991**, *52/53*, 35.
(30) Kimura, T.; Choppin, G. R. *J. Alloys Compd* **1994**, *213/214*, 313.
(31) David, F. H.; Fourest, B. *New J. Chem.* **1997**, *21*, 167.
(32) Yamaguchi, T.; Nomura, M.; Wakita, H.; Ohtaki, H. *J. Chem. Phys.* **1988**, *89*, 5153.
(33) Solera, J. A.; Garca, J.; Proietti, M. G. *Phys. Rev. B* **1995**, *51*, 2678.
(34) Allen, P. G.; Bucher, J. J.; Shuh, D. K.; Edelstein, N. M.; Reich, T. *Inorg. Chem.* **1997**, *36*, 4676.
(35) Conradson, S. D. *Appl. Spectrosc.* **1998**, *52*, 252A.
(36) Bucher, J. J.; Edelstein, N. M.; Osborne, K. P.; Shuh, D. K.; Madden, N.; Luke, P.; Pehl, D.; Cork, C.; Malone, D.; Allen, P. G. *SRI 95 Conf. Proc., Rev. Sci. Instrum.* **1996**, *67*, 1.

at ~200 kHz per channel, and the spectra were corrected for detector deadtime using a 2 μs time constant. XAFS data reduction, which included analysis of both the extended X-ray absorption fine structure (EXAFS) and the X-ray absorption near-edge structure (XANES) spectral regions, was performed by standard methods described elsewhere[37] using the package of programs EXAFSPAK developed by G. George of SSRL. Multiple XAFS scans (2−6, 40 min each) were collected from each sample at ambient temperature (~25 °C), and the results were averaged. The spectra were energy calibrated by simultaneous measurement of the spectrum of the appropriate trivalent elements aquo reference solution. For samples which did not transmit X-rays (e.g., Ln^{3+} ions at high Cl^- concentration), the spectra were self-calibrated on the absorption edge of the Ln^{3+} ion under investigation. The energies of the first inflection points for the reference sample absorption edges, E_r, were defined at 5483 eV (La^{3+} L_{III}), 5723 eV (Ce^{3+} L_{III}), 6208 eV (Nd^{3+} L_{III}), 7613 eV (Eu^{3+} L_{II}), 8944 eV (Yb^{3+} L_{III}), 17038 eV (Y^{3+} K-edge), 18504 eV (Am^{3+} L_{III}), and 18970 eV (Cm^{3+} L_{III}). When appropriate, XAFS data were acquired at the L_{II}-edge to avoid monochromator crystal glitches encountered immediately above the L_{III}-edge. The EXAFS threshold energies, E_0, were defined as 5500, 5740, 6225, 7630, 8964, 17055, 18520, and 18990 for the La^{3+}, Ce^{3+}, Nd^{3+}, Eu^{3+}, Yb^{3+}, Y^{3+}, Am^{3+}, and Cm^{3+} edges, respectively. Nonlinear least-squares curve-fitting for the raw k^3-weighted EXAFS data were done using the EXAFSPAK programs.

The EXAFS data were fit using theoretical phases and amplitudes calculated from the program FEFF7 of Rehr et al.[38] All of the spectra were modeled using single scattering (SS) M−O and M−Cl paths derived from the hypothetical cluster MO_7Cl^{2+} embedded in a MO_2 extended lattice (fluorite structure) where M refers to the specific metal ion being analyzed. The embedded cluster method increases the effective lattice size and reduces problems associated with discontinuities in overlapping atomic potentials for smaller basis sets. The FEFF7 phases and amplitudes were refined by performing initial curve-fits to a given data set and repeating the FEFF7 calculation using bond lengths adjusted appropriately with the scale factor (RMULT) option. S_0^2, the amplitude reduction factor, was held fixed at 1.0 in each of the fits. The shift in threshold energy, ΔE_0, was allowed to vary as a global parameter in each of the fits (i.e., the same ΔE_0 was used for each shell). An initial inspection of the curve-fits revealed that changes in the data sets as a function of increased chloride concentration could be modeled primarily with changes in the coordination numbers of O and Cl, (N_O and N_{Cl}). Values were chosen for σ based on curve fits to the spectra of the free aquo ions (at low Cl^-). Thus, σ^2 was held constant for La, Ce, Nd, and Eu−O at 0.0090 Å^2, and for Yb and Y−O at 0.0080 Å^2 (the smaller value is due to shorter, tighter bond lengths). The value of $\sigma^2 = 0.0050$ Å^2 for the Cl^- shell was taken from earlier work.[34] Consequently the fits were highly constrained by holding the Debye−Waller factor, σ, constant, which avoids correlation problems between N and σ and establishes more consistently the changes in coordination number as a function of Cl^- concentration.

Analysis of the early Ln^{3+} ion EXAFS required special care due to the presence of glitch-like features present in the spectra. These sharp transitions in the EXAFS region of Ln $L_{III,II}$-edges have been documented and assigned as multielectron excitations (MEE) of the $N_{V,IV}$-edges according to the $Z + 1$ model of double excitations.[33] Their intensity is strongest for La^{3+} and diminishes as one goes across the lanthanide series. Due to their sharpness, the features were treated as glitches and removed from the data prior to spline fitting. However, the uncertainty in accurate treatment of these spectral contaminations adds a degree of uncertainty to the EXAFS curve-fitting results which will be discussed later.

Results

La^{3+} EXAFS. Figure 1 shows the La L_{III}-edge EXAFS and corresponding Fourier transforms (FTs) for the La^{3+} ion in 0.25 M HCl and 14 M LiCl. The results of the curve-fits are also shown in Figure 1 and tabulated in Table 1. The EXAFS data only extend out to $k = 9.2$ Å^{-1} due to the onset of the L_{II}-edge. This however only limits the attainable resolution for shells of identical near-neighbors ($\Delta R = (\pi/2k_{max}$ where $\Delta R = R_2 - R_1$) and does not diminish the ability to discern the presence of Cl^- backscattering in the first shell. At low molar Cl^- concentration, the EXAFS data depict the structure of the free aquo ion with 9.2 ± 1.5 water molecules at 2.54 ± 0.02 Å in the first coordination sphere. Due to the short k-range, curve-fits cannot confirm or disprove the presence of specific structures such as a 9-coordinate, tricapped trigonal prism possessing two different first shell O distances with $\Delta R \leq 0.16$ Å. Our result is comparable with the coordination environment of 8 waters at 2.57 Å found for La^{3+} by X-ray scattering.[39]

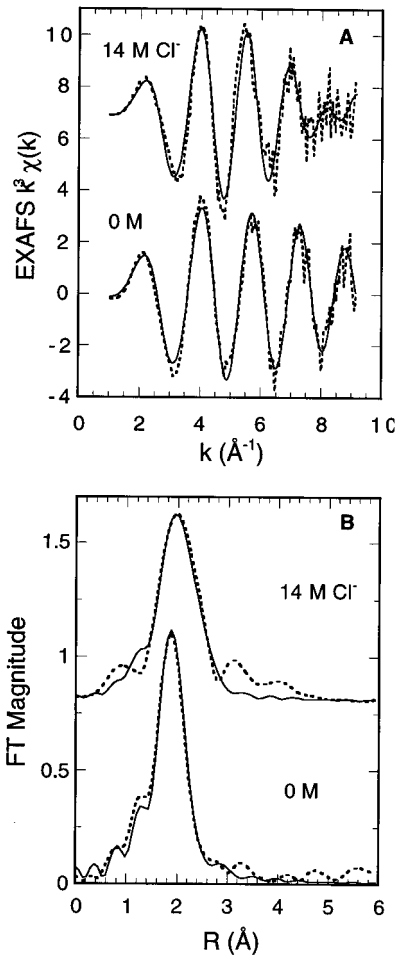

Figure 1. Raw La L_{III}-edge k^3-weighted EXAFS data (A) and corresponding Fourier transforms (B) taken over $k = 1-9.2$ Å^{-1} for La^{3+} in 0.2 and 14 M Cl^-: experimental data (•••), theoretical fit (—).

The spectra at 14 M LiCl show dramatic changes both in k-space and in the FTs. There is an obvious change in phase of the sine wave to a higher frequency oscillatory pattern. The FTs demonstrate this more clearly as the main peak (uncorrected for the EXAFS phase shift, $\alpha \approx -0.5$ Å) shifts to higher R. Although there is only one main peak observed in the FT, curve-fits indicate the presence of 7.0 ± 1.5 water molecules at 2.54 ± 0.02 Å and 2.4 ± 1.5 Cl^- ions at 2.92 ± 0.02 Å. EXAFS in principle cannot distinguish between O and N or Cl and S neighbors (due to similar Z), but the knowledge of the chemistry in these systems limits the possible configurations. The presence

(37) Prins, R.; Koningsberger, D. E. *X-ray Absorption: Principles, Applications, Techniques for EXAFS, SEXAFS, and XANES*; Wiley-Interscience: New York, 1988.
(38) Rehr, J. J.; Mustre de Leon, J.; Zabinsky, S.; Albers, R. C. *Phys. Rev. B* **1991**, *44*, 4146.
(39) Johansson, G., Wakita, H. *Inorg. Chem.* **1985**, *24*, 3047.

Table 1. Lanthanide EXAFS Curve-Fitting Summary

		Ln−O		Ln−Cl				
ion	medium	R (Å)	$N^{a,b}$	R (Å)	$N^{a,b}$	ΔE_0	k-range	F-values[c]
La^{3+}	0.25 M HCl	2.54	9.2			−7.3	1−9.2	
	14.0 M LiCl	2.57	6.5	2.92	2.1	−6.8	1−9.2	0.69/0.38
Ce^{3+}	0.25 M HCl	2.52	9.3			−8.8	1−9.3	
	14.0 M LiCl	2.56	7.3	2.89	1.8	−7.1	1−9.3	0.75/0.42
Nd^{3+}	0.25 M HCl	2.49	9.5			−8.2	1−9.5	
	14.0 M LiCl	2.51	7.8	2.85	1.9	−6.8	1−9.5	0.53/0.22
Eu^{3+}	0.25 M HCl	2.43	9.3			−5.9	1−9.9	
	14.0 M LiCl	2.46	8.2	2.81	1.1	−6.1	1−9.9	0.41/0.24
Yb^{3+}	0.25 M HCl	2.32	8.7			−2.4	1−13	
	13.3 M LiCl	2.33	8.6			−3.5	1−13	
	6 M LiCl/MeOH	2.34	3.9	2.60	3.3	−1.4	1−12	
Y^{3+}	0.25 M HCl	2.36	9.7			−7.3	1−13	
	12.5 M LiCl	2.36	9.6			−8.5	1−13	

[a] The standard deviations (1σ) for R and N as estimated by EXAFSPAK are as follows: Ln−O, $R \pm 0.003$ Å and $N \pm 0.37$; An−Cl, $R \pm 0.005$ Å and $N \pm 0.2$. [b] σ^2 held constant for La, Ce, Nd, and Eu−O at 0.0090 Å^2; Yb and Y−O at 0.0080 Å^2; and Ln−Cl at 0.0050 Å^2. [c] F-values shown are for (1 O shell fits)/(1 O shell + 1 Cl shell fits) to indicate relative improvements in the goodness of fit, see ref 40 for a description. Fits to the 0.25 M data sets which included a Cl shell offered no improvement in the F-values, see Supporting Information.

of the Cl^- ion was confirmed by comparing the fit minimization F-values[40] from EXAFSPAK for 1 shell fits (O only) with those of 2 shell fits (O and Cl). The absence of Cl in the 0.25 M fits was confirmed in a similar fashion (see Supporting Information).

Ce^{3+}, Nd^{3+}, and Eu^{3+} EXAFS. Proceeding across the lanthanide series, a structural trend is revealed regarding the onset of chloride complexation and replacement of water molecules within the Ln^{3+} ion inner coordination spheres. Going from Ce^{3+} to Eu^{3+} in 14 M LiCl, the values of N_{Cl} decrease from 1.8 to 1.1 ± 0.6 Cl^- ion and the water coordination numbers increase from 7.3 to 8.2 ± 0.7. Evidence for the lanthanide contraction is observed in the Ln^{3+}−O bond lengths at 0.25 M HCl, which decrease from 2.52 Å for Ce^{3+} to 2.43 Å for Eu^{3+}. The tendency for Cl^- to replace water in the inner sphere is decreasing as the lanthanide ionic radii decrease. The EXAFS data for Eu^{3+} (see Supporting Information) display effects similar to the data for La^{3+}; however, the effect is considerably weaker. Although the Eu^{3+} EXAFS phase shifts in k and R-space are difficult to discern in the 14 M solution relative to the 0.025 M solution, the curve-fitting results in Table 1 indicate a statistically significant improvement in the fit quality with the inclusion of a Cl^- shell in the 14 M LiCl data set.[34,40] The effect of Cl^- complexation on the Nd^{3+} ion was readily detected in the EXAFS, and the values for N_{Cl} and N_O follow the absolute trend noted here.

Yb^{3+} and Y^{3+} EXAFS. The trend of weaker Cl^- ion inner sphere complexation at 14 M LiCl going across the lanthanide series apparently continues to the point where Cl^- does not enter the inner sphere of the Yb^{3+} ion. The EXAFS data and corresponding FTs for Yb^{3+} in 0.25 M HCl and 13.3 M LiCl, shown in Figure 2, are virtually identical. The curve-fitting results (Table 1) indicate the presence of 8.7 O at 2.32 Å and 8.6 O at 2.33 Å for the 0.25 M HCl and 13.3 M LiCl solutions, respectively. No significant improvement in the fit to the 13.3 M data set was observed with the inclusion of a second shell of Cl^- ions. An analogous result was obtained for the Y^{3+} ion, which showed 9.7 O at 2.36 Å and 9.6 O at 2.36 Å for 0.25 M HCl and 12.5 M LiCl solutions, respectively. In addition to the lack of inner sphere chloride complexation for both the Yb^{3+} and Y^{3+} ions, perhaps the more interesting result is the absence of any detectable dehydration at high ionic strength. Since these ions have similar ionic radii yet different electronic structure, the stability of their respective aquo complexes in ~14 M LiCl (relative to the formation of chloro complexes in the early lanthanides) must be dominated by ionic interactions rather than orbital overlap or electronic properties. One method which

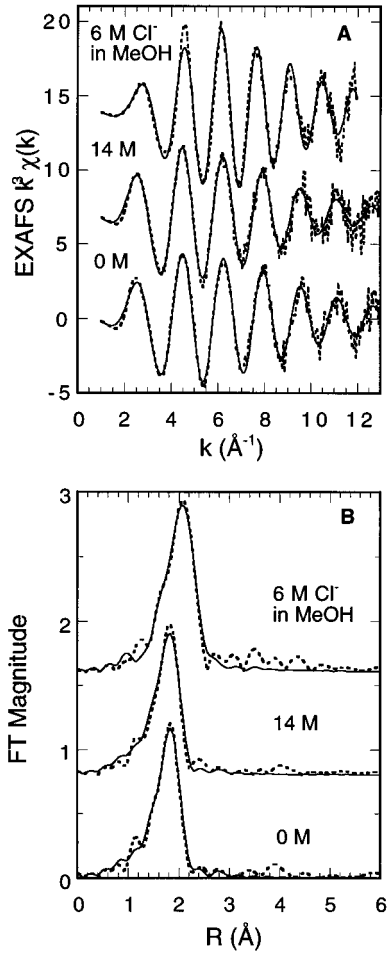

Figure 2. Raw Yb L_{III}-edge k^3-weighted EXAFS data (A) and corresponding Fourier transforms (B) taken over $k = 1-13$ Å^{-1} for Yb^{3+} in 0.2 and 13.3 M Cl^-, and in 6 M LiCl methanol solution: experimental data (···); theoretical fit (—).

(40) F is a goodness of fit parameter defined as $F = \sum k^6(\text{data} - \text{fit})^2/(N_{pts} - N_{var})$ where N_{pts} is the number of data points and N_{var} is the number of floating variables. The ratio of F-values obtained with and without the inclusion of a Cl^- (or O) shell of atoms is used here to quantify the fit improvement with Cl^- in the endpoint spectra (i.e., Cl^- detection limits at high Cl^- concentration).

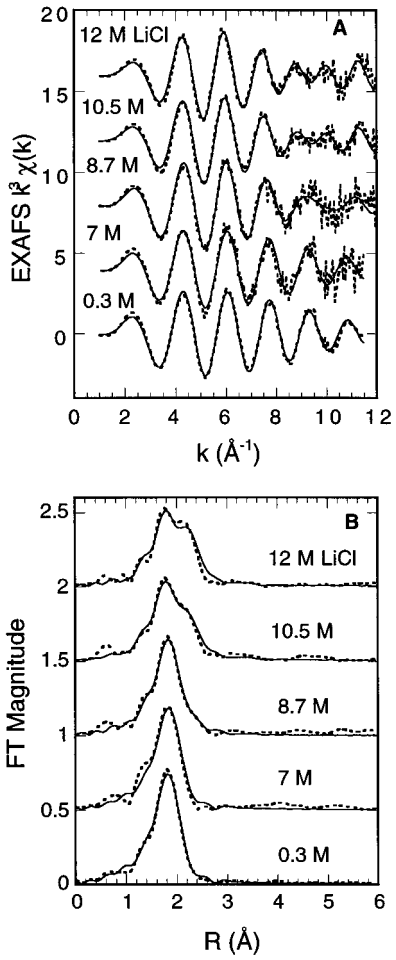

Figure 3. Raw Cm L_{III}-edge k^3-weighted EXAFS data (A) and corresponding Fourier transforms (B) taken over $k = 1-11$ Å^{-1} for Cm^{3+} as a function of [Cl^-]: experimental data (···); theoretical fit (—).

proved to be effective in dehydrating these ions and promoting significant inner sphere Cl^- ion complexation was to prepare the solutions in a matrix of >95% methanol. Figure 2 also shows the EXAFS data for Yb^{3+} in a methanol solution containing 6.0 M LiCl. Curve fitting for this data set indicates 3.9 O at 2.34 Å and 3.3 Cl^- at 2.60 Å, and this result was used as a reference point in analyzing for chloride complexation in the aqueous solutions.

Pu^{3+}, Am^{3+}, and Cm^{3+} EXAFS. The EXAFS spectra for the Cm^{3+} ion as a function of chloride concentration are shown in Figure 3. Similar results were obtained for Am^{3+} and are given in the Supporting Information. In 0.25 M HCl, the data for these ions are dominated by a single frequency, indicative of inner sphere water molecule coordination. The structures of the Am^{3+} and Cm^{3+} aquo ions as determined by the curve fits (Table 2) are 10.3 O at 2.48 Å and 10.2 O at 2.45 Å, respectively. For comparison, the relevant curve fitting results from earlier work[34] on Pu^{3+} in 0.25 and 12.5 M Cl^- were adjusted using $S_0^2 = 1$ and are presented in Table 2 along with the results for Am^{3+} and Cm^{3+}. The oxygen coordination numbers of 9.2, 10.3, and 10.2 are in general agreement and within experimental error. However, their average value is higher than the number of 8−9 reported by Conradson et al.[35] The decrease in An^{3+}−O bond lengths for the aquo complexes with increasing Z is consistent with the well-documented contraction of the actinide ionic radii across the series.

On increasing LiCl concentration, there is a noticeable change in the EXAFS frequency at ca. $k = 9$ Å^{-1}. This change is more pronounced for Cm^{3+} than for Am^{3+} and signifies the presence of a second absorber−scatterer interaction whose EXAFS wave is interfering with that of the oxygen atoms. Curve-fits indicate that this interaction is due to Cl^- entering the inner sphere of these ions (Table 2). The effect is seen more readily in the FTs (Figure 3B and Supporting Information) where the peak broadens and shifts to higher R. Since N_{Cl} is higher for Cm^{3+} than for Am^{3+} (2.4 vs 1.8, $N \pm 0.3$ at the 95% confidence limit) and the data set extends out to a higher k-range, we are able to resolve two distinct peaks in the FT of the Cm^{3+} ion in 12 M LiCl.

Ln^{3+} and An^{3+} XANES. It is appropriate to comment on the behavior of the XANES data that correspond to the EXAFS spectra discussed above. In analogy to results from our earlier work,[34] the XANES spectra of the trivalent ions are indeed sensitive to changes in the inner sphere ligation (i.e., chloride replacement of water). The spectra for each ion at high versus low chloride concentrations (see Supporting Information) show systematic changes in the intensities of the absorption edge features. For the Ln^{3+} ions which showed Cl^- ligation in 14 M LiCl, there is a concurrent change in a XANES feature (possibly a multiple scattering resonance) which occurs immediately after the main absorption peak (white line). Consistent with the EXAFS results and these observations, the Yb^{3+} ion XANES data showed no change in 14 M LiCl. For the An^{3+} ions, the change in XANES with increasing chloride concentration is manifested primarily by a decrease in the white line intensity. The changes seen in these spectra show strong sensitivity to changes in the local coordination structure and serve to corroborate the results obtained from the EXAFS curve-fitting analysis. Theoretical modeling is required to extend these interpretations and make detailed spectral assignments in the XANES region.

Discussion

The EXAFS results for Pu^{3+}, Am^{3+}, and Cm^{3+} ions in ~12 M LiCl suggest a trend of increasing chloride complex formation across this part of the actinide series. This result appears to be directly *opposite* to that observed in the lanthanide series (Figure 4). Not only does Pu^{3+} show no inner sphere chloride complexation, it also showed significant dehydration at high ionic strength (due to the strongly decreasing water activity) with N_O decreasing from 9.2 to 5.2. Although this is not surprising in terms of expected thermodynamic behavior at high ionic strength, the result for Pu^{3+} is intriguing since none of the trivalent lanthanide ions reported in this paper show any evidence for major changes in the total first shell coordination (i.e., the sum of the H_2O and Cl^- coordination numbers is essentially constant).

Fanghänel et al.[5] have determined the formation constants (β_1 and β_2) by measuring the optical spectra of Cm^{3+} as a function of the $CaCl_2$ concentration by time-resolved laser fluorescence (TRLF). Their spectroscopic measurements covered the range of molalities of $CaCl_2$ from 2.272 to 6.031. The N_{Cl} values obtained from EXAFS for Cm^{3+} at high LiCl concentration have been correlated to the N_{Cl} values derived from the data of Fanghänel et al.[5] In order to place the data from two aqueous chloride solutions on a common scale, we have correlated the concentrations and mean ionic activities of LiCl and $CaCl_2$ with the activity of water, a_{H_2O}, in these systems. From the TRLF study of Fanghänel et al., we have taken the relative concentrations of the species Cm^{3+}, $CmCl^{2+}$, and

Table 2. Actinide EXAFS Curve-Fitting Summary

		An−O		An-Cl				
ion	medium	R (Å)	$N^{a,b}$	R (Å)	$N^{a,b}$	ΔE_0	k-range	F-ratio[c]
Pu^{3+}	0.01 M LiCl	2.51	9.2			−10.4	1−9.5	
	12.3 M LiCl	2.50	5.2			−7.3	1−9.5	1.0
Am^{3+}	0.25 M HCl	2.48	10.3			−8.7	1−11	
	8.0 M LiCl	2.49	8.9			−7.1	1−11	
	10.0 M LiCl	2.48	7.6	2.80	1.2	−7.3	1−11	0.17/0.06
	12.5 M LiCl	2.51	6.4	2.81	1.8	−6.1	1−11	0.23/0.08
Cm^{3+}	0.25 M HCl	2.45	10.2			−13.0	1−11.5	
	7.0 M LiCl	2.46	9.3			−11.7	1−11.5	
	8.7 M LiCl	2.45	8.2	2.76	1.2	−12.0	1−12.2	0.34/0.21
	10.5 M LiCl	2.44	6.6	2.75	2.1	−14.2	1−12.0	0.32/0.09
	12.3 M LiCl	2.45	6.1	2.76	2.4	−13.5	1−12.2	0.32/0.11

[a] The standard deviations (1σ) for R and N as estimated by EXAFSPAK are as follows: An−O, $R \pm 0.002$ Å and $N \pm 0.33$; An−Cl, $R \pm 0.006$ Å and $N \pm 0.1$. [b] σ^2 held constant for Pu−O at 0.010 Å^2; Am and Cm−O at 0.0090 Å^2; and Am and Cm−Cl at 0.0050 Å^2. [c] F-values shown are for (1 O shell fits)/(1 O shell + 1 Cl shell fits) to indicate relative improvements in the goodness of fit, see ref 40 for a description. Fits to the 0.25 M HCl data sets which included a Cl shell offered no improvement in the F-values.

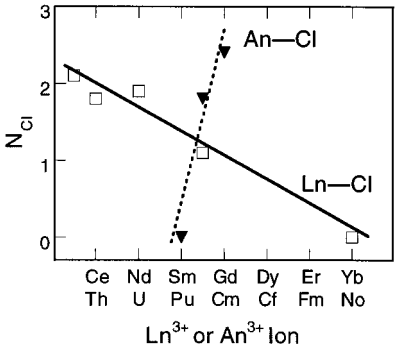

Figure 4. Chloride coordination numbers, N_{Cl}, in ca. 14 M LiCl solutions vs Ln(III) and An(III) atomic numbers.

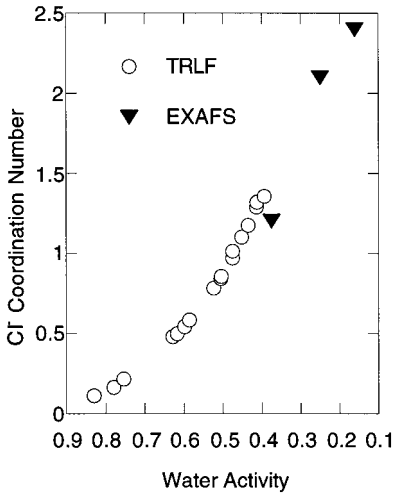

Figure 5. Average chloride coordination numbers, N_{Cl}, as a function of water activity, a_{H_2O}, for the Cm(III) ion. The data at low chloride concentration (high a_{H_2O}) shown by circles are calculated from the TRLF study of Fanghänel et al.,[4] and the data shown by the solid triangles are taken from the EXAFS results described in this paper.

$CmCl_2^+$ to calculate the effective value of N_{Cl}. Figure 5 shows a plot of N_{Cl} vs water activity for both the TRLF and EXAFS results. There is good agreement between the two measurements at the point where $a_{H_2O} \approx 0.4$. The values of N_{Cl} obtained from the EXAFS data extend up to much higher Cl^- activity (lower a_{H_2O}) and fall in a region of the plot which would coincide with a curve extrapolated from the TRLF values.

The chloride complexes formed for the trivalent actinide and lanthanide series at high LiCl concentrations represent extreme conditions since the mean ionic chloride activity of 12 M LiCl is about 620. Surprisingly, even with this mean ionic activity Pu^{3+} shows no chloro complexation. Marked changes in the ultraviolet absorption spectra of aqueous concentrated LiCl solutions of Pu^{3+} previously have been interpreted as due to the formation of the inner sphere $PuCl_2^+$ complex. Our EXAFS data do not confirm this result. The heavier actinides, Am^{3+} and Cm^{3+}, do show inner sphere chloro complexation under these extreme conditions. Our EXAFS data corroborate the inner sphere speciation model used to analyze the Cm^{3+} spectroscopic data in aqueous $CaCl_2$ solutions. The question remains as to the source of the changes in the f^n to $f^{n-1}6d$ spectra of Pu^{3+} in aqueous LiCl solutions.[13] The EXAFS data suggest that this could be due to the loss of H_2O molecules from the inner sphere due to decreasing water activity as the LiCl concentration increases. However, it has been reported that in 10 M perchloric acid solutions, where the H_2O activity is similar to that of concentrated LiCl solutions, no significant effects on the optical spectrum of Np^{3+} were observed.[14,41] Thus the reason for the changes in the optical spectra of Pu^{3+} with increasing LiCl concentration remains an open question.

For Cm^{3+} at 7.0 M LiCl (mean ionic activity ∼45), we are unable to observe any chloro complexation. However, at 8.7 M LiCl (mean ionic activity ∼120) we observe an average coordination number for all the inner sphere chloro complexes in solution of 1.2 ± 0.33 (1σ). These data suggests that at low LiCl concentrations (∼5 M or less) little inner shell chloride complexation occurs. If we assume that the trivalent lanthanide ions which show chloro complexation at higher concentrations of LiCl are similar to Cm^{3+} (and Am^{3+}), we then conclude that these trivalent lanthanide ions also have no significant inner shell chloride complexation at chloride concentrations of ∼5 M or less. This conclusion is supported by other studies using different techniques.[42,43]

From the above arguments we conclude that measurements of trivalent lanthanide and actinide formation constants for chloro complexation in relatively dilute solutions (<5 M) must be due to outer sphere complexation. We assume that our present results can be used to infer relative trends in stability for inner shell chloride complexes across the Ln^{3+} and An^{3+} series. Then assuming stepwise complex formation, the observation that the chloride coordination numbers at a given ionic strength decrease across the trivalent lanthanide series as a function of atomic

(41) Sjoblom, R.; Hindman, J. C. *J. Am. Chem. Soc.* **1951**, *73*, 1744.
(42) Yaita, T.; Ito, D.; Tachimoro, S. *J Phys. Chem. B* **1998**, *102*, 3886.
(43) Choppin, G. R.; Peterman, D. R. *Coord. Chem. Rev.* **1998**, *174*, 283.

number indicates that the stability constants (formation of a mono- or dichloro complex) are becoming smaller. This trend has been documented earlier as the stability constants selected by Martell et al. give values of log β_1 decreasing from -0.1 for La to -0.4 for Lu.[1c] Similarly, the observation that the Cl^- coordination numbers at a given ionic strength increase for Pu^{3+}, Am^{3+}, and Cm^{3+} suggests that the stability constants for these ions are becoming larger. The trend of increasing log β_1 values for chloride complexation with Pu, Am, and Cm has also been documented previously by Fanghänel et al.[5] in their tabulation of stability constants which were obtained from spectroscopy-based methods.

An important issue discussed in the Introduction is that of accuracy and precision in determining the water (O) coordination numbers for all of the trivalent pure aquo ions (in the absence of Cl^-). The EXAFS results presented here indicate water coordination numbers in 0.2 M HCl ranging from 8.7 to 9.5 for the Ln^{3+} ions. One source of uncertainty arises from a statistical treatment of the goodness-of-fit data within EXAFSPAK, where the estimated standard deviations are obtained from the diagonal elements of the covariance matrix. At the 95% confidence limit, the uncertainty in N_O for all Ln^{3+} ions is ± 1.1. The variations in N_O observed across the early Ln^{3+} ion series represent another source of uncertainty which is best described in terms of precision. Considering the values of N_O obtained for La^{3+}, Ce^{3+}, Nd^{3+}, and Eu^{3+} only (which are expected to be ~ 9 from previous reports), we can use these values as a test of the reproducibility in our measurements and subsequent analyses. Taking the average for all of these ions gives $N_O = 9.3$ with an uncertainty of ± 0.4 (95% confidence limit). Since the La^{3+}, Ce^{3+}, Nd^{3+}, and Eu^{3+} EXAFS were all treated by the same FEFF7 and EXAFSPAK modeling procedures (i.e., identical model calculation, σ^2, and S_0^2 values), the precision is governed primarily by the variations in the anomalous MEE feature, slight differences in the *k*-ranges, noise statistics, and other experimental errors.

A comparison between these methods of error treatment reveals the benefits of taking multiple measurements. If we were to rely solely on the statistical analysis from a single curve fit, we would conclude that EXAFS spectroscopy cannot distinguish unambiguously between $N_O = 8$ or 9 for the Ln^{3+} ions. If on the other hand we were to choose to use the reproducibility, which in this case has a smaller standard deviation, we might conclude that EXAFS can in fact distinguish between $N_O = 8$ or 9 for these Ln^{3+} L-edge spectra.

The key problem is that of absolute accuracy, which is dictated largely by the modeling approaches employed. At present, it is necessary to make estimates of important amplitude factors (i.e., σ^2 and S_0^2) due to a lack of appropriate solution model compounds (solid state structures are not appropriate). These uncertainties in addition to other systematic errors both in the experimental measurement and data reduction (pre-edge and spline fitting) will also contribute to the absolute error. The presence of asymmetry in the first coordination sphere may also contribute to modeling uncertainties. However, recent EXAFS results on tetravalent actinide aquo ions suggests that the use of an asymmetrical distribution for σ^2 offers negligible improvement over the symmetric Gaussian pair distribution in these pure aquo ion systems.[44]

It is possible that potential systematic errors in modeling are indeed observed in our results. For example, the average N_O for the early Ln^{3+} ions is lower than that for the An^{3+} ions (9.3 vs 9.9), and the average N_O for Yb^{3+} is lower than that of the Y^{3+} ion (8.7 vs 9.7). In each of these comparisons, the bond lengths, σ^2, S_0^2, and the FEFF7 model calculation were nearly identical. An explanation for the differences may include some combination of the following possibilities: (1) the assumption that the ions have the same σ^2 or S_0^2 factors is incorrect; (2) there are differences in the FEFF7 calculations for Ln^{3+} L-edges, An^{3+} L-edges, and the Y^{3+} K-edge which are not taken into account here; (3) the measurements or data reduction techniques are systematically different; and (4) the differences in N_O are real. Further work is necessary from a detailed theoretical standpoint to address these important issues.

Acknowledgment. This work was supported by the Director, Office of Energy Research, Office of Basic Energy Sciences, Chemical Sciences Division of the U.S. Department of Energy, under Contract No. DE-AC03-76SF00098, and by Lawrence Livermore National Laboratory under Contract No. W-7405-ENG-48. The authors are indebted for the use of ^{243}Am and ^{248}Cm materials to the Division of Chemical Sciences, Office of Basic Energy Sciences, through the transplutonium element production facilities at Oak Ridge National Laboratory. This work was done (partially) at SSRL, which is operated by the Department of Energy, Division of Chemical Sciences. The authors also acknowledge the key efforts of the EH&S personnel from LBNL, SLAC, and SSRL.

Supporting Information Available: Figures of Eu and Am EXAFS spectra and corresponding fits, selected XANES spectra, and additional curve-fitting details. This material is available free of charge via the Internet at http://pubs.acs.org.

IC9905953

(44) Moll, H.; Denecke, M. A.; Jalilehvand, F.; Sandstrom, M.; Grenthe, I. *Inorg. Chem.* **1999**, *38*, 1795−1799.